American Mineralogist, Volume 79, pages 809–818, 1994

Mechanism of CO_3^{2-} substitution in carbonate-fluorapatite: Evidence from FTIR spectroscopy, ^{13}C NMR, and quantum mechanical calculations

P. Regnier,* A. C. Lasaga, R. A. Berner**
Department of Geology and Geophysics, Yale University, New Haven, Connecticut 06511, U.S.A.
O. H. Han,† K. W. Zilm
Department of Chemistry, Yale University, New Haven, Connecticut 06511, U.S.A.

Abstract

The substitution of CO_3^{2-} in carbonate-fluorapatite ("francolite") has a destabilizing effect on the apatite structure that results in increased solubility. A commonly proposed substitution mechanism involves the replacement of a PO_4^{3-} ion by CO_3F^{3-}, in which C is at the center of a tetrahedron and is surrounded by three O atoms and one F atom at the corners. However, no spectroscopic evidence exists for this hypothetical anion.

We have investigated the microenvironment of CO_3^{2-} in ^{13}C-enriched type B synthetic and natural sedimentary carbonate-fluorapatite samples by ^{13}C static and MAS NMR and FTIR spectroscopies. (True CO_3^{2-} substitution in the apatite structure was ascertained by X-ray diffraction and FTIR.) The CO_3^{2-} ion itself consists of an sp^2-hybridized planar arrangement of three O atoms about the central C atom. If the CO_3^{2-} geometry were changed to an sp^3 hybrid with F^- at one corner, the NMR chemical isotropic shift would change considerably, owing to the altered environment about the central C atom. Also, there would be an internuclear dipolar interaction between ^{13}C and ^{19}F.

Simulated NMR spectra for ^{13}C-^{19}F distances of 1.38 and 2.00 Å based on the sp^3 model are very different from those obtained on our apatite samples, which are instead characteristic of C in a planar sp^2 arrangement and no ^{13}C-^{19}F dipolar coupling. No evidence for direct bonding between CO_3^{2-} and F was found. This result is confirmed by ab-initio quantum mechanical calculations, which show that the hypothetical CO_3F^{3-} ion is unstable in an apatitic environment. Ab-initio results, as well as FTIR data, favor the existence of an interstitial position for F^- if nonstoichiometric amounts of this element are present in apatite.

Introduction

The most abundant authigenic phosphate phase in marine sediments is a highly substituted form of fluorapatite, carbonate-fluorapatite, also known as "francolite" (McConnell, 1973; Jahnke, 1984). It is well established that carbonate substitution has a destabilizing effect on the apatite structure resulting in increased solubility (Chien and Black, 1976; Vieillard, 1978; Jahnke, 1984). The concentration variations of structure-bound CO_3^{2-} in carbonate-fluorapatite have also been interpreted as diagenetic or paleoenvironmental indicators (for an extensive review, see Schuffert et al., 1990). However, the true crystal chemical nature of this substitution is still controversial.

The association of the CO_3^{2-} ions with apatites has been investigated by many methods (Beshah et al., 1990): X-ray diffraction, chemical analyses, infrared and Raman spectroscopy, electron paramagnetic resonance, and proton and ^{13}C NMR. However, most of these studies have been carried out for medical purposes on pure synthetic hydroxylapatite, bone tissues, or dental enamel, i.e., in F-poor environments.

From chemical studies and mineralogical data of sedimentary apatites, Borneman-Starinkevich and Belov (1953), Elliott (1964), Smith and Lehr (1966), Trueman (1966), Guldbrandsen (1966), McClellan and Lehr (1969), and Binder and Troll (1989) have suggested that when a planar CO_3^{2-} ion substitutes for a tetrahedral PO_4^{3-} group, the vacant O site is occupied by a F ion. The mechanism is also supported by Bacquet et al. (1980) from EPR experiments. This CO_3F^{3-} arrangement would preserve electroneutrality and complete the coordination of the cations in the structure. However, these results seem to be ambiguous. Okazaki (1983) and Jahnke (1984) found no clear positive relationship between the fluoride content and the amount of CO_3^{2-} incorporated during apatite precipitation. Furthermore, natural carbonate-fluorapatite formation takes place in a complex ionic environment, and the electroneutrality of the crystal structure could be maintained by several other chemically simpler

* Present address: Department of Chemical Oceanography, University of Brussels, CP208, 1050 Brussels, Belgium.
** To whom reprint requests should be sent.
† Present address: Korea Basic Science Center, Yoosung-goo, Yeueun-dong 224-1, Taejon 305-333, South Korea.

0003–004X/94/0910–0809$02.00

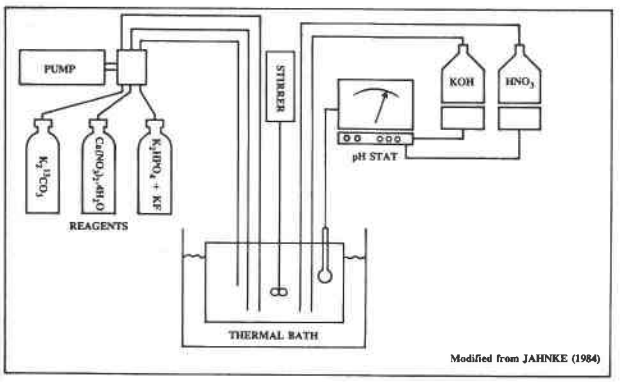

Fig. 1. Experimental system used in the pH-stat precipitation experiments. See text for details.

substitution mechanisms. For example, replacement of Ca^{2+} by Na^+ (LeGeros et al., 1968; McClellan and Lehr, 1969; Bonel et al., 1973; Nelson and Featherstone, 1982; Driessens et al., 1983) and lattice defect formation (Bonel et al., 1973; Tochon-Danguy et al., 1980) have been extensively studied.

Direct spectroscopic evidence for the existence of this hypothetical CO_3F^{3-} ion is essentially missing. The aim of this paper is to identify the microenvironment of CO_3^{2-} existing in synthetic and natural sedimentary carbonate-fluorapatite, using FTIR spectroscopy, ^{13}C NMR spectroscopy, and quantum mechanical calculations.

Samples

Synthetic samples were prepared using the pH-stat apparatus of Van Cappellen and Berner (1991). The system was modified to follow the experimental method of Jahnke (1984).

A plastic vessel containing 1 L of reaction solution was stirred by a suspended magnetic stir bar to avoid the grinding of crystals against the bottom of the vessel (Fig. 1). Temperature was maintained at 70 °C. A Ross combination pH electrode with an internal reference was coupled with an automatic titrator that delivers either a concentrated KOH solution or a concentrated HNO_3 solution to maintain a constant solution pH. During the experiments, fluctuations in pH were kept within 0.05 units (Van Cappellen and Berner, 1991).

Reagents in the form of 0.2 *M* $Ca(NO_3)_2 \cdot 4H_2O$, 0.12 *M* K_2HPO_4 with 0.048 *M* KF solution, and 0.0027 *M* $K_2{}^{13}CO_3$ were added to the reaction vessel by means of peristaltic pump at a rate of 8 mL/h. Dramatic variations in ionic strength were avoided by using 0.1 *M* KNO_3 solution as the reaction medium (Jahnke, 1984). KNO_3 was used because K^+ substitutes into apatite to a much lesser extent than Na^+ (Bonel et al., 1973; Jahnke, 1984). After 24 h, the addition of reagents by means of the peristaltic pump was stopped, and the precipitate was allowed to equilibrate for an additional 5 h; it then was filtered, washed with distilled H_2O, and dried at room temperature. The pH of the experiment was maintained at 6.95 to avoid precipitation of other minerals, especially calcite.

The phosphorite analyzed in this study was a phosphate sample from the Babcock Deep core, located in southwestern Florida, furnished by John Compton of the University of South Florida. The chemical composition of the carbonate-fluorapatite from this sample, given by Compton (personal communication), is $(Ca_{4.50}Mg_{0.06}Na_{0.20}Sr_{0.01})(PO_4)_{2.17}(CO_3)_{0.57}(SO_4)_{0.18}F_{0.97}$.

Experimental methods

Chemical analysis

Ca and P from the synthetic sample were analyzed by inductively coupled plasma-emission spectroscopy (ICP Varian Liberty-200) after the dissolution of the synthetic sample in dilute acid. Fluoride content was determined by ion-selective electrode. K incorporation in the crystals was checked by electron microprobe analysis using crystal dispersion (PET crystal, 15 kV, 10^{-8} A). Under such conditions, the minimum concentration of certain detection for K is approximately 0.1%.

X-ray diffraction and infrared spectroscopy

The samples were checked by X-ray diffraction to confirm the mineral identity and the crystallinity of the material. The apatites were scanned on a Scintag Pad-V diffractometer (Cu$K\alpha$, 45 kV, 40 mA). The CO_3^{2-} content of carbonate-fluorapatite was determined from measurements of the $\Delta 2\theta$ for either the 004-410 or the 300-002 pair of reflections. This method relies upon an empirical equation to convert the $\Delta 2\theta$ measurement to a CO_3^{2-} concentration (Guldbrandsen, 1970; Schuffert et al., 1990). The experimental conditions and the relationship given by Schuffert et al. (1990) were used for our calculations: $y = 10.643x^2 - 52.512x + 56.986$, where $y = CO_3^{2-}$ wt% and $x = \Delta 2\theta$ (004-410).

In addition to the $\Delta 2\theta$ measurements, XRD was also used to check each sample for the presence of calcite. The peak of highest intensity for this mineral occurs at approximately 29.4° 2θ. Under the conditions employed (Schuffert et al., 1990), the detection limit is approximately 1.0 wt%.

The infrared spectra were obtained using KBr pellets; 5 and 15 mg of sample were mixed in an agate mortar with 1 g of KBr. Transparent pellets were obtained under vacuum at a pressure of 200 kg/cm^2. The FTIR spectra were recorded using a Brucker IFS25 apparatus.

Nuclear magnetic resonance

All the experiments were carried out on a homemade spectrometer with a magnetic field strength of 7.05 T (Larmor frequency: ^{13}C = 75.648 MHz). The nuclear magnetic resonance (NMR) instrument is equipped with a Tecmag data system and an Oxford Instruments 89-mm bore superconducting solenoid. A magic angle spinning (MAS) multinuclear resonance probe (Doty Scientific, Inc.) was used for ^{13}C MAS NMR experiments (1.1%

abundance, $I = ½$). Sapphire rotors, of 7-mm outer diameter, were spun at 4–4.8 kHz. The MAS spin rates were measured before and after each experiment electronically. A homemade static probe was employed to acquire static-echo spectra.

In all experiments, spin-echo sequences and phase cycling of the pulses were used to suppress pulse breakthrough and other artifacts (Stejskal and Schaefer, 1974). For MAS, a spin echo with the π pulse timed to occur exactly one rotor period after the initial $\pi/2$ pulse was employed. If the echo sequence is not synchronous with the sample rotation, the spin echo and the MAS can interfere, resulting in the destruction of the signal (Maricq and Waugh, 1979; Olejniczak et al., 1984). All echo signals were acquired in quadrature, with the carrier placed close to the center of gravity of the resonance. A typical $\pi/2$ pulse length was 6 μs.

Chemical shifts reported here are all relative to external tetramethylsilane (TMS), with downfield shifts taken as positive, and have a precision of about 1 ppm.

Ab-initio quantum mechanical calculations

Investigation of the bonding and atomic dynamics of minerals can answer significant questions concerning the stability of a crystal structure (e.g., Sauer, 1989; Lasaga and Gibbs, 1989). The bulk of the ab-initio work has effectively emphasized the use of suitable molecular clusters to replace the infinite periodic structure of a mineral.

In our simple cluster model, geometric optimization of a central ion (either PO_4^{3-} or CO_3F^{3-}) through energy minimization was performed in a point-charge array that mimics the spatial atomic distribution in the apatite structure. These calculations were carried out with the Gaussian-90 (Frish et al., 1990) computer program using several basis sets to expand the molecular orbitals. A basis set is defined by the linear combination of atomic orbitals, which are usually themselves expanded in terms of Gaussian functions. The geometric optimization was handled by the Fletcher-Powell method (Fletcher and Powell, 1963). In this case, the gradient of the SCF energy, which is the first derivative of the energy with respect to displacement in the nuclear coordinates, is evaluated numerically (Hehre et al., 1986).

Results and discussion

Chemical analysis

The stoichiometric formula of the synthetic sample, given in ions per unit cell and normalized to ten Ca atoms is: $Ca_{10}(PO_4)_{5.64}(CO_3)_{0.244}(F,OH)_{2.587}(H_2O)_{4.18}$. OH ions were determined from charge balance conditions and account for 27% occupancy of the monovalent positions. (H_2O content was calculated from the mass balance requirement.) Trace amounts of K (<0.1%) in the sample were neglected in these calculations. CO_3^{2-} content was calculated from the $\Delta 2\theta$ of the 004-410 diffraction peaks.

The Ca:PO_4:F,OH molar ratio of the synthetic carbonate-fluorapatite indicates an excess of monovalent anions from the stoichiometry of pure apatite (10:6:2).

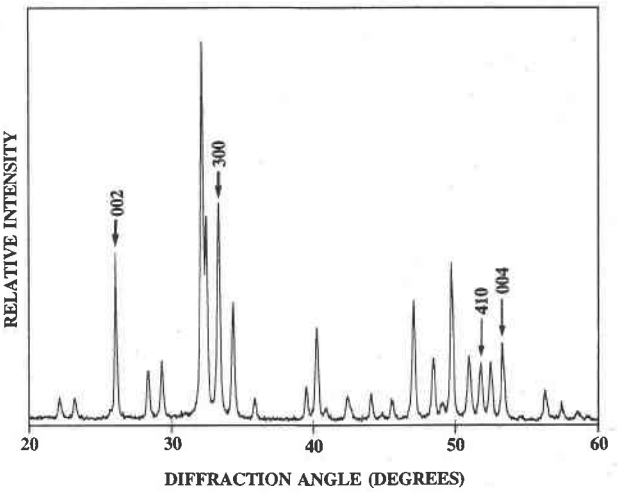

Fig. 2. X-ray diffraction scan of the synthetic carbonate-fluorapatite at 1° 2θ/min using a Scintag Pad-V diffractometer. The angular distance between the 410-004 and 002-300 diffraction peaks is used to determine the carbonate content of the apatite sample.

X-ray diffraction

The X-ray diffractogram of the synthetic carbonate-fluorapatite is shown in Figure 2. The presence of other mineral phases is unlikely, since every peak is accounted for by the apatite structure. Most important, the sample did not contain any crystalline calcium carbonate. The CO_3^{2-} content of the synthetic sample determined from the relationship given by Schuffert et al. (1990) is 1.36 ± 0.61 wt%. The relatively small amount of CO_3^{2-} incorporated in the synthetic sample can be correlated with the almost neutral pH at which the experiment was conducted (Jahnke, 1984).

A fast scan of the natural sample has also been performed. The XRD measurement indicates that this sediment is a mixture of quartz and well-crystallized phosphorite grains.

FTIR spectroscopy

Figure 3A shows the infrared absorption spectrum of synthetic carbonate-fluorapatite in the region 1600–400 cm^{-1}. The same domain was also covered at a lower sensitivity (Fig. 3B). The ν_1 mode of the PO_4^{3-} ion is represented in apatites by a very narrow band (965 cm^{-1}), and the ν_2 mode produces an absorption peak at 470 cm^{-1} (Fig. 3A). As shown by Rey et al. (1991), the main absorbance signal of PO_4^{3-} appears in the triply degenerate ν_3 domain (Fig. 3B). Finally, the ν_4 mode gives two main bands at 600 and 560 cm^{-1} and a shoulder at 575 cm^{-1} (Fig. 3A, 3B). The anisotropic electric field of crystalline apatite splits the degeneracy of this absorption band into a well-defined doublet, and a high crystallinity index (CI = 5.1) was extracted from the amount of splitting (Termine and Posner, 1966; Rey et al., 1990; Shemesh, 1990). No additional bands are present in either the ν_3 or ν_4

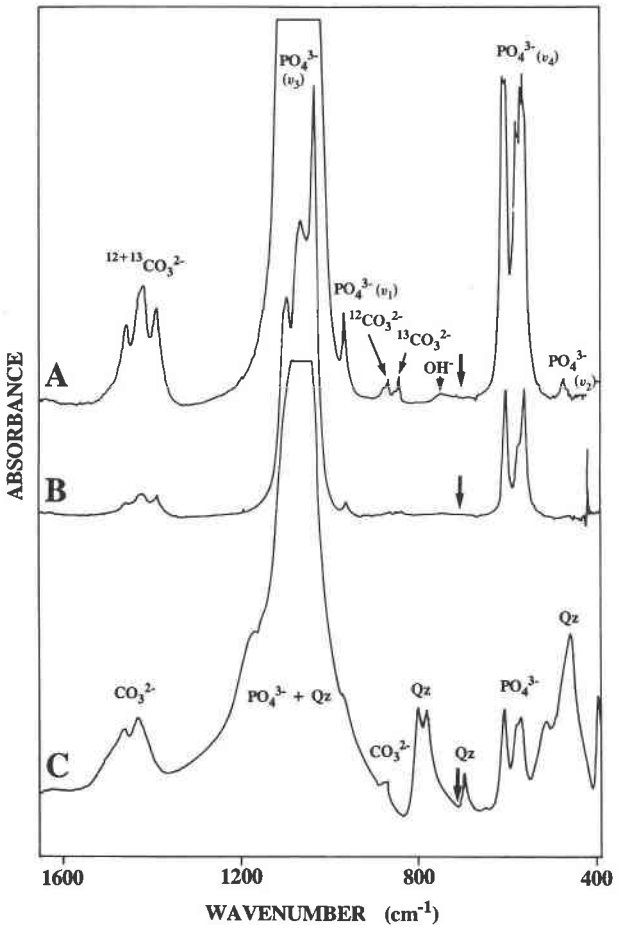

Fig. 3. Fourier transform infrared (FTIR) spectra of (A) synthetic carbonate-fluorapatite (~15 mg sample per g KBr); (B) synthetic carbonate-fluorapatite (~5 mg sample per g KBr); (C) natural carbonate-fluorapatite. Qz are the SiO_4^{4-} vibrational modes attributed to quartz. The absence of the C-O absorption bands at about 710 cm^{-1} (thick arrows) in the spectra of both samples indicates that no detectable $CaCO_3$ is associated with the marine apatites. The detailed structure of the CO_3^{2-} vibrational bands are discussed in Fig. 4.

domains, and, therefore, no distinguishable nonapatitic environments or ions (e.g., HPO_4^{2-} ions) are present in the precipitated mineral phase.

The IR spectrum of the natural sample is shown in Figure 3C. The broad peak at around 1000 cm^{-1} is due to both the ν_1-ν_3 PO_4^{3-} modes and the most intense SiO_4^{4-} absorption band. The ν_2 PO_4^{3-} signal is also masked by another quartz peak, and the only well-defined PO_4^{3-} band is thus the doubly degenerate ν_4 mode. The well-defined doublet at 798–779 cm^{-1} and the band at 695 cm^{-1} are all attributed to the presence of quartz in this sample.

Finally, a very weak band at 740 cm^{-1} is observed in Figure 3A, which can be attributed to the substitution of F by OH ions in synthetic fluorapatite (Freund and Knobel, 1977; Klee, 1974; Baumer et al., 1985, 1990). The presence of some OH^- groups is confirmed by a faint absorption band at 3570 cm^{-1} (not shown in Fig. 3).

Among the four internal vibrational modes of the free CO_3^{2-} ion, only two are of importance for IR investigations in calcium phosphates: ν_2 and ν_3 (Rey et al., 1989). The absence of the C-O absorption bands at about 710 cm^{-1} in the spectrum (identified by heavy arrows in Fig. 3) indicates that no detectable $CaCO_3$ is associated with our synthetic carbonate-fluorapatite (LeGeros et al., 1980). This confirms our XRD results.

Both ^{12}C and ^{13}C were incorporated into apatite during the precipitation experiments. During the experiments, the natural CO_3^{2-} initially dissolved in the reaction vessel was progressively diluted by ^{13}C, which was added as $K_2{}^{13}CO_3$ solution. The ν_2 peak at 875 cm^{-1}, which is caused by the $^{12}CO_3^{2-}$ out-of-plane stretching mode is therefore shifted to 850 cm^{-1} for the $^{13}CO_3^{2-}$ incorporated in the apatite structure (Fig. 4E). Another pair of peaks due to ^{12}C and ^{13}C appears at 865 and 840 cm^{-1}, respectively. The ratios of observed frequencies (875/850 = 1.0294, 865/840 = 1.0298) are in good agreement with the expected value of 1.029 calculated from the reduced masses of ^{12}C and ^{13}C (Doi et al., 1982). The ν_3 mode at ~1400–1500 cm^{-1}, corresponding to the strongest IR peaks of the ion is composed of three bands (Fig. 4E). Doi et al. (1982) observed the $^{12}CO_3$ peaks in hydroxylapatite at 1410 and 1460 cm^{-1} and at 1380 and 1420 cm^{-1} for $^{13}CO_3$. Therefore, the medium wavenumber component obtained in our synthetic sample is probably a composite peak of the 1410 and 1420 cm^{-1} absorption bands.

The ν_2 and ν_3 CO_3^{2-} bands of the natural carbonate-fluorapatite are both well characterized and respectively appear at 866 and 1428/1458 cm^{-1} (Fig. 4F). Synthetic and natural carbonate-fluorapatite thus have a very similar CO_3^{2-} signal.

Furthermore, the shape of the ν_3 signal and the absence of C-O absorption bands at 710 cm^{-1} also clearly indicate that no detectable calcite is associated with the natural carbonate-fluorapatite sample.

The infrared spectrum of the CO_3^{2-} ion in apatite has been explained by the presence of carbonate ions in two environments (Elliott, 1964; Bonel, 1972a, 1972b). It is now widely accepted that CO_3^{2-} substitutes either for the column anions OH^- and F^- or for PO_4^{3-} ions in the apatite structure. This substitution in two different crystallographic sites results in two sets of absorption bands corresponding to type A CO_3^{2-} substitution (1540–1460–878 cm^{-1}, Fig. 4B) and type B CO_3^{2-} substitution (1455–1420–871 cm^{-1}, Fig. 4A). An extensive review of the literature shows, however, that the precise IR peak positions vary sometimes significantly (Elliott, 1964; Montel, 1973; Bacquet et al., 1980; Tochon-Danguy et al., 1980; Nelson and Featherstone, 1982; Doi et al., 1982; Driessens et al., 1983; Okazaki, 1983; Elliott et al., 1985; Vignoles et al., 1988; Rey et al., 1989; Baumer et al., 1990).

The characteristic absorption of type A CO_3^{2-} at 1540 cm^{-1} is absent from the spectrum of both synthetic (Fig.

4E) and natural (Fig. 4F) samples, which clearly indicates that no CO_3^{2-} is incorporated in the column anion sites. By contrast, the ν_3 mode of type B apatite (Fig. 4A) is clearly exhibited by both the synthetic and natural samples.

The interpretation of the ν_2 CO_3^{2-} band is more complex. Rey et al. (1989) found a band at 871 (Fig. 4A) and 878 cm^{-1} (Fig. 4B) for type B and type A hydroxylapatite samples, respectively. However, the origin of the 878-cm^{-1} band is still the center of several controversies. Nelson and Featherstone (1982) effectively showed that it also appeared in apatites without the ν_3 spectral characteristics of type A CO_3^{2-}. They consequently attributed this band to a second kind of type B CO_3^{2-}. The same spectra (a band at 878 cm^{-1} without the presence of a band at 1540 cm^{-1}: Fig. 4C) were later obtained by Rey et al. (1989) for synthetic hydroxylapatite and are in good agreement with the results obtained for the synthetic apatite (Fig. 4E). These ν_2 spectral characteristics are lacking for the natural sample, and, in this case, the only observed component is found at 866 cm^{-1} (Fig. 4F).

Another interesting feature of Figure 4 is the slight displacement of the ν_2 peak positions toward lower wavenumbers (878 → ~874 cm^{-1}; 871 → 866 cm^{-1}) related to an increase in the degree of sample fluoridation (compare Fig. 4C with Fig. 4D). It is thus normal that the values obtained in our study (875, and 865 cm^{-1} for the synthetic sample, 866 cm^{-1} for the natural carbonate-fluorapatite) are displaced with respect to the positions generally accepted for hydroxylapatite (Fig. 4A–4C). Since it is well known that absorption bands can be broadened, split, or shifted by mutual interactions of adjacent ions or combination with low wavenumber lattice vibrations, Okazaki (1983) speculated that F^- greatly affects the neighboring ions. Vignoles (1984), on the basis of a semi-quantitative study of the IR spectra, identified these two type B CO_3^{2-} peaks as CO_3^{2-}-□ (O vacancy) and CO_3^{2-}-F^- associations. However, LeGeros et al. (1968) and Rey et al. (1989) found these data to be ambiguous and simply attributed the shifting of the 878- and 871-cm^{-1} bands of nonfluoridated apatites to a change of composition.

Nuclear magnetic resonance spectroscopy

The static-echo spectra of both samples are shown in Figure 5. The spectrum of 10% ^{13}C enriched $BaCO_3$ is shown in Figure 5C for comparison. The spectrum has a typical line shape due to an axially symmetric chemical-shift anisotropy (Abragam, 1961). The center of gravity and singularities of the pattern can be regarded as a fingerprint for CO_3^{2-} ions (Duncan, 1990). (The humps near 30 ppm, marked by stars in Figure 5A and 5B, are from the parafilm used to cap the sample tubes.) The line widths become broader in the following order: $BaCO_3$, synthetic apatite, and natural apatite. However, the MAS spectra of the two apatite samples have an identical isotropic chemical shift of 170 ± 1 ppm, as shown in Figure 6. (The peaks near 115 ppm are background signals from the probe and kel-F rotor caps.) One of the two spinning side-band peaks of the apatites happens to appear at the

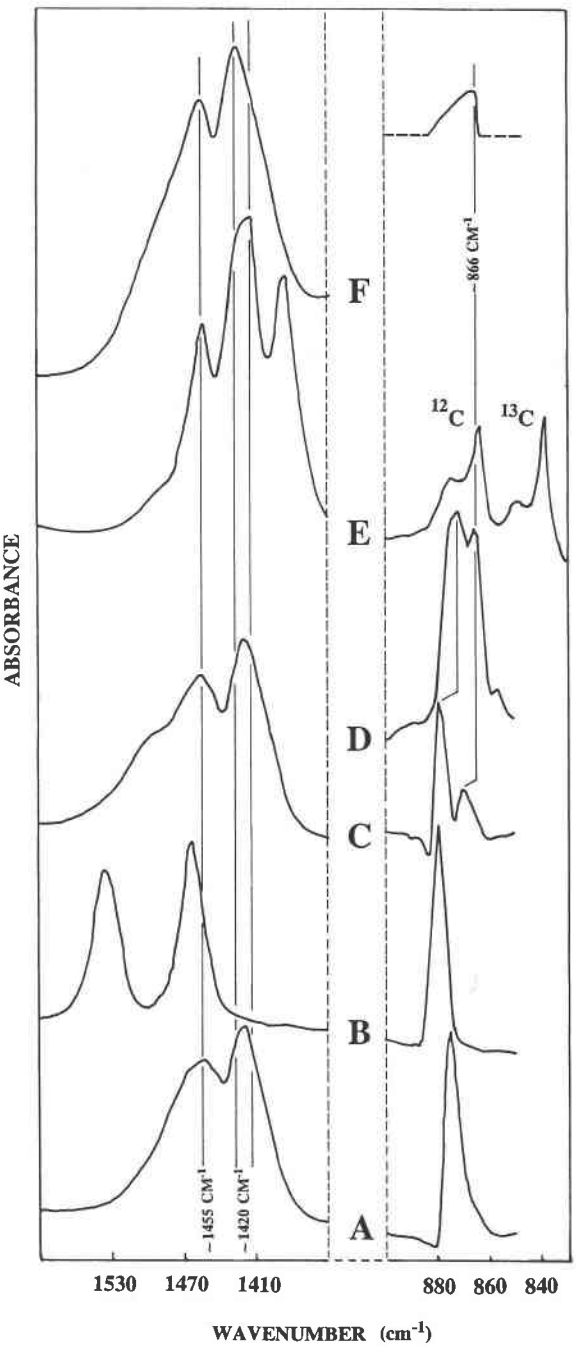

Fig. 4. FTIR spectra of CO_3^{2-} vibrational bands in carbonate-fluorapatite samples. (A) type B carbonate hydroxylapatite; (B) type A carbonate hydroxylapatite; (C) hydroxylapatite without the usual type A location band at 1540 cm^{-1} but with an 878-cm^{-1} band; (D) a fluoridation experiment showing the ν_2 CO_3^{2-} vibrational band shift; (E) synthetic apatite from the present study; (F) marine carbonate-fluorapatite from the present study. See text for a complete description. Data for curves A–D are from Rey et al. (1989).

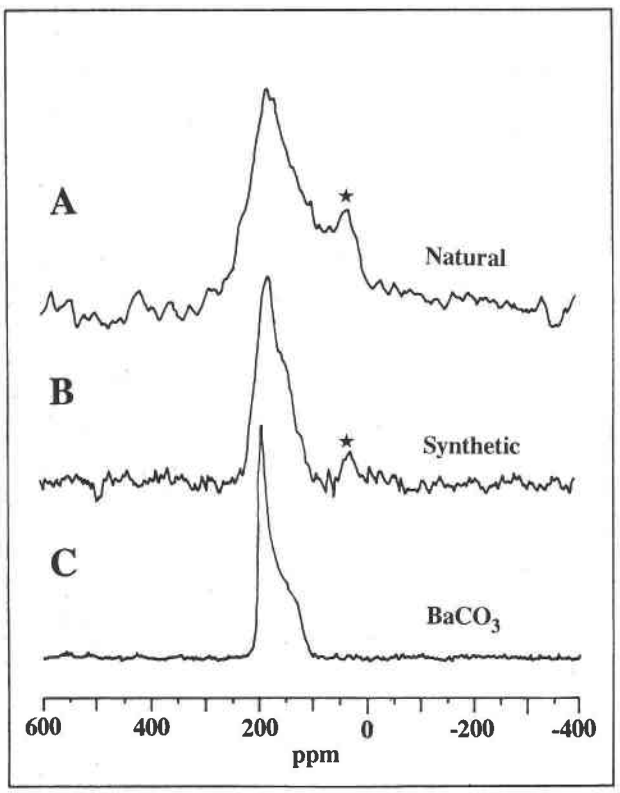

Fig. 5. (A) The static-echo spectrum of the natural apatite sample, with 1.5-s repetition time, 27200 scans, and line broadening of 800 Hz. (B) The static-echo spectrum of the synthetic apatite sample, with 60.5-s repetition time, 688 scans, and line broadening of 400 Hz. (C) The static-echo spectrum of the 10% ^{13}C-enriched $BaCO_3$ sample, with 60.5-s repetition time, 16 scans, and line broadening of 200 Hz. Stars represent the background signal from the Parafilm.

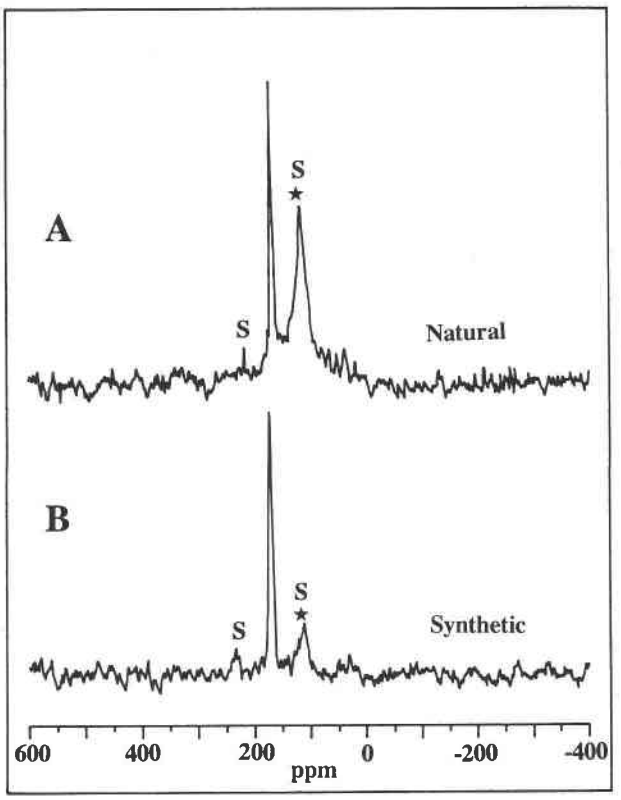

Fig. 6. (A) The MAS spectrum of the natural apatite sample at 4.0 kHz, with 2.5-s repetition time, 16512 scans, and line broadening of 200 Hz. (B) The MAS spectrum of the synthetic apatite sample at 4.68 kHz, with 30.5-s repetition time, 1632 scans, and line broadening of 200 Hz. Stars represent the background signal from kel-F rotor caps and the stator of the probe; S notifies spinning side-band peaks.

same chemical shift with the background peaks so that it is obscured by the background signals. The line widths of the central peaks in the MAS spectra are not much different, even though those in the static spectra are. Actually, the line width of the MAS spectrum of the natural apatite sample is narrower than that of the MAS spectrum of the synthetic sample.

The CO_3^{2-} ion consists of a central sp^2 hybridized C atom, with three O atoms at the corners of an equilateral triangle. The three O atoms are about 2.3 Å apart, with a C-O distance of about 1.29 ± 0.02 Å (Tossel and Vaughan, 1992), and the whole group lies in a plane at right angles to the threefold c axis.

Since O has a low abundance of the magnetic isotope ^{17}O (0.037%, $I = 5/2$), with a small magnetogyric ratio [-3.6279×10^7 rad/(T·s)] and a large quadrupole moment (-2.6×10^{26} Q/m^2), the dipolar interaction between the O atoms and C is negligible. The C NMR spectra of carbonates would be expected to be dominated by the chemical-shift anisotropy, but C spectra of carbonates have been observed to be unaffected upon exchange of countercations (Duncan, 1990).

The spectra of our apatite samples are principally that of CO_3^{2-}, as supported by the observed isotropic chemical shift of 170 ± 1 ppm in the MAS spectra. The overall line shapes in the static spectra are also consistent with that of $BaCO_3$ in Figure 5C, which implies that both samples have the same chemical-shift anisotropy as $BaCO_3$.

The line broadening due to dipolar interactions and paramagnetic impurities in the natural sample results in a broader line width in the static spectrum than that for the synthetic sample. By contrast, the line width of the MAS spectrum of the natural sample (Fig. 6A) is narrower than that of the synthetic sample (Fig. 6B). The line width of the MAS spectrum is determined mainly by the distribution of isotropic shifts and other residual interactions, since chemical shift anisotropy is averaged out by MAS and would not contribute to line broadening (Maricq and Waugh, 1979; Herzfeld and Berger, 1980). Therefore, this difference in line width suggests that the distribution of isotropic chemical shifts due to different microscopic environments is greater in the synthetic sample. In addition, the static spectrum of the synthetic sample (Fig. 5B) has poor singularities of the chemical-shift

anisotropy powder pattern compared with the $BaCO_3$. These results suggest that there is a distribution of chemical-shift anisotropy patterns even with the same isotropic chemical shift. Thus, the synthetic apatite is not as crystalline as the $BaCO_3$ sample. On the other hand, XRD and IR results show that the synthetic apatite is very well crystallized. These contradictory results imply that CO_3^{2-} defect sites in the synthetic apatite have a range of variation of structural distortion of the CO_3^{2-} and of orientation in the crystal, even though this apatite is well crystallized overall.

If the CO_3^{2-} is at the center of a tetrahedron, with the O atoms at the three corners of the tetrahedron and one F atom at the other corner (e.g., Borneman-Starinkevich and Belov, 1953; Elliott, 1964; Smith and Lehr, 1966; Trueman, 1966; Guldbrandsen, 1966; McClellan and Lehr, 1969; Bacquet et al., 1980; Binder and Troll, 1989), the isotropic chemical shift is expected to be different, since the hybridization of the C center would no longer be sp^2. In addition, if F were so close to the central C atom, the spectrum would be governed not only by the chemical-shift anisotropy of C but also by a dipolar interaction between C and F. The simulated spectra for C-F distances of 1.38 and 2.00 Å, shown in Figure 7B and 7C, are very different from that for a planar CO_3^{2-} in Figure 7A and different from our results shown in Figure 5. When the C-F distance is 3.00 Å, the spectrum (Fig. 7D) becomes similar to that of the pure carbonate. However, it is difficult for the C in the apatite to have a bond with F at this or a longer distance without perturbing the local structure severely. Also, the contribution of the dipolar interactions between C and other nuclei (for example, P) at 3 Å or a longer distance would be on the same order of magnitude as that of C and F as an isolated pair of dipoles. Therefore, it would not be justified to use the model of an isolated dipole pair to simulate the spectra with 3 Å or a longer distance.

In summary, our NMR results (Fig. 5) show that C in both apatite samples has three O atoms at the corners of a planar equilateral triangle (Fig. 7A) without direct bonding with a F atom (Fig. 7B, 7C). Analogous results were obtained by Beshah et al. (1990) for CO_3^{2-} containing hydroxylapatite using CP-MAS ^{13}C and ^1H NMR. They found no evidence for the presence of CO_3OH^{3-} as a substituting ion.

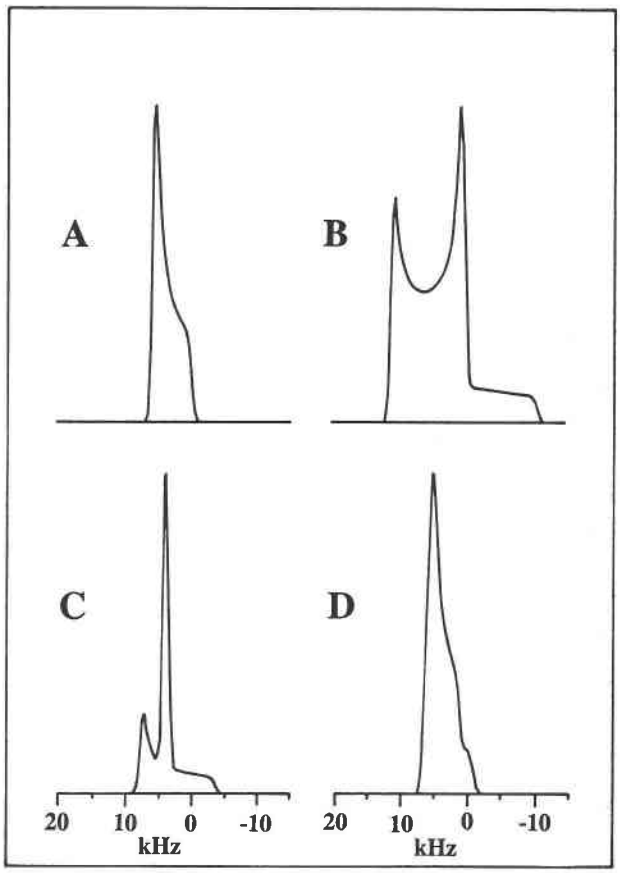

Fig. 7. (A) The simulated static-echo spectrum of a C atom in CO_3^{2-} in a planar equilateral triangle with no dipole interaction. (B) The simulated static-echo spectrum of a C atom in CO_3^{2-}, with F at a distance of 1.38 Å. Both the chemical-shift anisotropy of a pure carbonate and the dipolar interaction between C and F are considered. The F is assumed to lie on a line that runs through the C atom in a carbonate group and is perpendicular to the plane of the CO_3^{2-} ion. (C) The simulated spectrum with the distance of 2.00 Å between C and F. (D) The simulated spectrum with the distance of 3.00 Å between C and F. A Gaussian line broadening of 500 Hz was applied to each spectrum.

Quantum mechanical calculations

Energy minimization by the Fletcher-Powell geometric optimization algorithm was carried out first on isolated PO_4^{3-} anions to test our simple model. Table 1 lists P-O bond lengths, O-P-O bond angles, and SCF energies at the optimized geometries as a function of the basis set. As already observed (O'Keeffe et al., 1985), it was necessary to use orbitals of higher angular momentum than required by the number of electrons in P (addition of polarization functions) to reproduce known geometries accurately.

The results obtained at the 3-21G* and 6-31G* levels were quite similar, and we selected the former basis set for subsequent optimizations, including an additional array of point ions (Fig. 8). An equal fractional charge was assigned to each surrounding atom to make up a net positive charge of +3 that balanced the charge of PO_4^{3-}. In this case, the energy minimum of the calculated system was found for coordinates that are in very good agreement with the positions generated from the unit-cell dimensions (Hughes et al., 1989) of the crystal (Table 1). Especially, a symmetry breakdown in bond length and bond angles that is consistent with experimental data is observed when a surrounding potential is taken into account.

The same procedure was subsequently used for a hypothetical CO_3F^{3-} anion. C-F bond length and electron

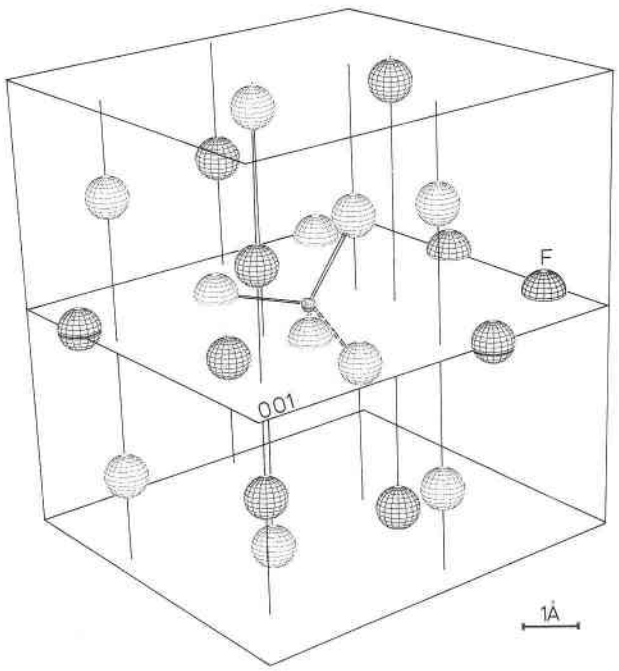

Fig. 8. Apatite molecular cluster centered around a fully optimized PO_4^{3-} ion. The nonphosphate atoms are generalized points of fractional charge, making up a net positive charge of +3 that balances the negative charge of the PO_4^{3-} ion. The vertical lines are parallel to the screw axis of the mineral and perpendicular to the (001) plane. O = open spheres, Ca = shaded spheres, F is represented by the letter F, and the P atom = the small sphere.

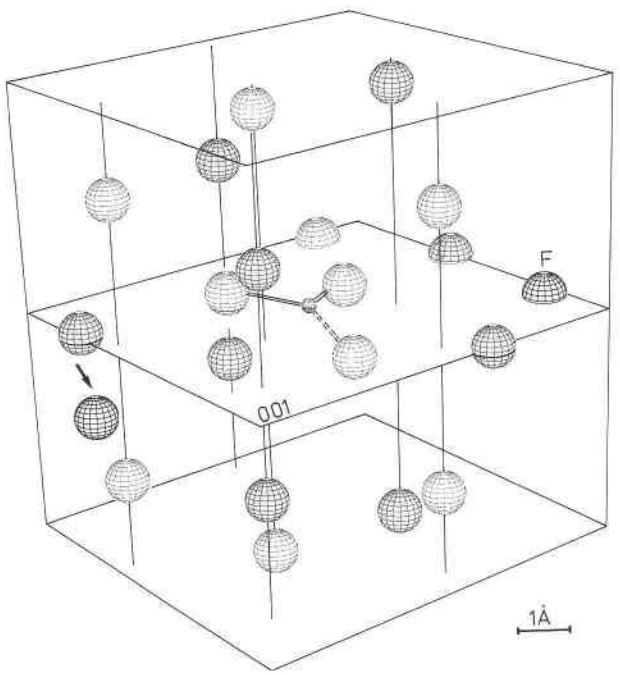

Fig. 9. Apatite molecular cluster after the replacement of PO_4^{3-} by CO_3F^{3-} (crystal orientation as indicated in Fig. 8). O = open spheres, Ca = shaded spheres, F is represented by the letter F, and the C atom = the small sphere. Note the interstitial position for F (thick arrow).

TABLE 1. P-O bond lengths, O-P-O angles, and SCF energies at the optimized geometries for PO_4^{3-} as a function of the basis set

Basis	Bond length (Å)	Bond angle (°)	SCF energy (Hartrees)
		Without lattice charges	
STO-3G	1.713	109.49	−630.83528
	1.712	109.52	
	1.713	109.43	
	1.713		
3-21G*	1.562	109.51	−636.39530
	1.561	109.45	
	1.562	109.45	
	1.562		
6-31G*	1.568	109.50	−639.70781
	1.567	109.45	
	1.568	109.45	
	1.568		
		With lattice charges	
3-21G*	1.560	109.18	−637.24840
	1.574	108.03	
	1.558	110.04	
	1.559		
		Observed	
	1.538	108.00	
	1.539	107.45	
	1.531	111.12	
	1.532		

Note: the observed values have been obtained from the unit-cell dimension of the apatite crystal (data from Hughes et al., 1989). One Hartree = 627 Kcal/mol.

overlap population calculated at the 3-21G and 6-31G* levels, respectively, are compared from the structure obtained after three Fletcher-Powell optimization cycles (Table 2). The results are qualitatively the same to justify the use of the computationally simpler 3-21G basis set.

The same three-dimensional array of equal lattice charges selected for PO_4^{3-} calculations was subsequently included in the quantum mechanical calculations. As shown in Table 2, no optimal structure is found, and direct bonding between CO_3^{2-} and F^- is lacking. This is demonstrated clearly by the large C-F distance (3.61 Å)

TABLE 2. C-F distances and electron overlap population obtained at nonoptimized geometries for a hypothetical CO_3F^{3-} ion

Basis	Cycles	C-F distance (Å)	C-F electron overlap population
		Without lattice charges	
3-21G	5	3.832	0.000420
	7	9.360	0
		With lattice charges	
6-31G*	3	2.575	0.088
3-21G	3	2.494	0.090
	5	2.808	0.036
	10	3.610	0.000653
	15	3.611	0.000659
	20	3.611	0.000647

Note: cycles are Fletcher-Powell cycles. Overlap populations are from Mulliken population analysis. See text for the complete description.

and by the electron overlap population from C and F, which indicates that the electron density between these ions is virtually equal to zero (Table 2). Obviously, the potential of the surrounding species deeply modifies the behavior of the F atom explicitly incorporated in the quantum mechanical calculations. If one takes into account an array of atomic charges, F^- is interstitially trapped inside the cluster of interest (Fig. 9). This structure was obtained from the almost constant atomic positioning observed during the last ten Fletcher-Powell cycles (Table 2) and not from an optimized geometry (the RMS force was still above the threshold value). The exact atomic distribution probably depends on the way the apatite cluster was constructed (size and charge assignment). Nevertheless, these results suggest that if excess F is incorporated during carbonate-fluorapatite precipitation, it will be preferentially located interstitially rather than in the remaining vacant site left from the CO_3^{2-} for PO_4^{3-} replacement. This interpretation is consistent with our FTIR results. The observed ν_2 CO_3^{2-} band shift (871 → 866 cm^{-1}) is too small to be attributed to the formation of a $^{[4]}CO_3F^{3-}$ ion. A better interpretation of the measurements involves a slight distortion of the crystal structure, resulting from the presence of interstitial F ions; this model could easily explain the small observed IR band shift.

Acknowledgments

Research support was provided by NSF grant OCE-9115569 (to R.A.B.) and DOE grant DE-FG22-91-PC91285 (to K.W.Z.). We thank John Compton of the University of South Florida for providing the natural carbonate-fluorapatite sample.

References cited

Abragam, A. (1961) The principles of nuclear magnetism, 599 p. Oxford University Press, New York.

Bacquet, G., Vo Quang Truong, Bonel, G., and Vignoles, M. (1980) Résonance paramagnétique éléctronique du centre F^+ dans les fluorapatites carbonatées de type B. Journal of Solid State Chemistry, 33, 189–195.

Baumer, A., Ganteaume, M., and Klee, W. (1985) Determination of OH ions in fluorapatite by infrared spectroscopy. Bulletin de Mineralogie, 108, 145–152.

Baumer, A., Caruba, R., and Ganteaume, M. (1990) Carbonate-fluorapatite: Mise en évidence de la substitution $2PO_4^{3-} \rightarrow SiO_4^{4-} + SO_4^{2-}$ par spectrométrie infrarouge. European Journal of Mineralogy, 2, 297–304.

Beshah, K., Rey, C., Glimcher, M.J., Schimizu, M., and Griffin, R.G. (1990) Solid state carbon-13 and proton NMR studies of carbonate containing calcium phosphates and enamel. Journal of Solid State Chemistry, 84, 71–81.

Binder, G., and Troll, G. (1989) Coupled anion substitution in natural carbon-bearing apatites. Contributions to Mineralogy and Petrology, 101, 394–401.

Bonel, G. (1972a) Contribution a l'étude de la carbonatation des apatites. I. Annales de Chimie, 7, 65–87.

——— (1972b) Contribution a l'étude de la carbonatation des apatites. II and III. Annales de Chimie, 7, 127–144.

Bonel, G., Labarthe, J.C., and Vignoles, C. (1973) Contribution a l'étude structurale des apatites carbonatees de type B. Colloques Internationaux du CNRS, 230, 117–125.

Borneman-Starinkevich, I.D., and Belov, N.V. (1953) Carbonate-apatites. Døklady Akademie Nauk SSSR, 90, 89–92.

Chien, S.H., and Black, C.A. (1976) Free energy of formation of carbonate apatites in some phosphate rocks. Soil Science Society of America Proceedings, 40, 234–239.

Doi, Y., Moriwaki, Y., Aoba, T., Takahashi, J., and Joshin, K. (1982) ESR and IR studies of carbonate-containing hydroxyapatites. Calcified Tissue International, 34, 178–181.

Driessens, F.C.M., Verbeeck, R.M.H., and Heijligers, H.J.M. (1983) Some physical properties of Na- and CO_3-containing apatites synthesized. Inorganica Chimica Acta, 80, 19–23.

Duncan, T.M. (1990) A compilation of chemical shift anisotropies, p. 36C. Farragut, Chicago, Illinois.

Elliott, J.C. (1964) The crystallographic structure of dental enamel and related apatites. Ph.D. thesis, University of London, London, England.

Elliott, J.C., Holcomb, D.W., and Young, R.A. (1985) Infrared determination of the degree of substitution of hydroxyl by carbonate ions in human dental enamel. Calcified Tissue International, 37, 372–375.

Fletcher, R., and Powell, M.J.D. (1963) A rapidly convergent descent method for minimization. The Computer Journal, 6, 163–168.

Freund, F., and Knobel, R. (1977) Distribution of fluorine in hydroxyapatite studied by infrared spectroscopy. Journal of the Chemical Society, Dalton Transactions, 1136–1140.

Frish, M.J., Head-Gordon, M., Trucks, G.W., Foresman, J.B., Schlegel, H.B., Raghavachari, K., Robb, M., Binkley, J.S., Gonzalez, C., Defrees, D.J., Fox, D.J., Whiteside, R.A., Seeger, R., Melius, C.F., Baker, J., Martin, R.L., Kahn, L.R., Stewart, J.J.P., Topiol, S., and Pople, J. A. (1990) Gaussian 90, Revision F. Gaussian, Inc., Pittsburgh, Pennsylvania.

Guldbrandsen, R.A. (1966) Chemical composition of phosphorites of the phosphoria formation. Geochimica et Cosmochimica Acta, 30, 769–778.

——— (1970) Relation of carbon dioxide content of apatite of the Phosphoria formation to regional facies. U.S. Geological Survey Professional Paper, 700-B, 9–13.

Hehre, W.J., Radom, L., Schleyer, P.R., and Pople, J.A. (1986) Ab-initio molecular orbital theory, 548 p. Wiley Interscience, New York.

Herzfeld, J., and Berger, E.A. (1980) Sideband intensities in NMR spectra of samples spinning at the magic angle. Journal of Chemical Physics, 73 (12), 6021–6030.

Hughes, J.M., Cameron, M., and Crowley, K.D. (1989) Structural variations in natural F, OH, and Cl apatites. American Mineralogist, 74, 870–876.

Jahnke, R.A. (1984) The synthesis and solubility of carbonate fluorapatite. American Journal of Science, 284, 58–78.

Klee, W. (1974) OH-Ionen in naturlichen Fluorapatiten. Neues Jahrbuch für Mineralogie Monatshefte, 3/4, 127–143.

Lasaga, A.C., and Gibbs, G.V. (1989) Ab-initio quantum mechanical calculations of water-rock interactions: Adsorption and hydrolysis reactions. American Journal of Science, 290, 263–295.

LeGeros, R.Z., Trautz, O.R., LeGeros, J.P., and Klein, E. (1968) Carbonate substitution in the apatite structure. Bulletin de la Société Chimique de France, special issue, 1712–1718.

LeGeros, R.Z., Vandemaele, K.H., Quirolgico, G.B., and LeGeros, D.J. (1980) Transformation of calcium carbonates and calcium phosphates to carbonate apatites: Possible mechanism for phosphorite formation. Proceedings of the 2nd International Congress on Phosphorus Compounds, Boston, IMPHOS (Paris), 41–57.

Maricq, M.M., and Waugh, J.S. (1979) NMR in rotating solids. Journal of Chemical Physics, 70, 3300–3316.

McClellan, G.H., and Lehr, J.R. (1969) Crystal chemical investigations of natural apatites. American Mineralogist, 54, 1374–1391.

McConnell, D. (1973) Apatite, its crystal chemistry, mineralogy, and geologic and biologic occurrences, 111 p. Springer-Verlag, Berlin.

Montel, G. (1973) Conceptions actuelles sur la structure et la constitution des apatites synthétiques comparables aux apatites biologiques. Colloques Internationaux du CNRS, 230, 13–18.

Nelson, D.G.A., and Featherstone, J.D.B. (1982) Preparation, analysis, and characterization of carbonated apatites. Calcified Tissue International, 34, S69–S81.

Okazaki, M. (1983) $F^-CO_3^{2-}$ interaction in IR spectra of fluoridated CO_3-apatites. Calcified Tissue International, 35, 78–81.

O'Keeffe, M., Domenges, B., and Gibbs, G.V. (1985) Ab-initio molecular